JOURNAL OF THERMOPHYSICS AND HEAT TRANSFER
Vol. 15, No. 1, January–March 2001

Technical Notes

TECHNICAL NOTES are short manuscripts describing new developments or important results of a preliminary nature. These Notes cannot exceed six manuscript pages and three figures; a page of text may be substituted for a figure and vice versa. After informal review by the editors, they may be published within a few months of the date of receipt. Style requirements are the same as for regular contributions (see inside back cover).

Surface Temperature Diagnostics Using Infrared Multiwavelength Radiation Method

Wenhua Zhao,* Kuo Tian,† Shuguang Zhu,† and Pin Lu‡
Tsinghua University,
100084 Beijing, People's Republic of China

Nomenclature

A	=	area of the target point on the specimen, m^2
C_1	=	first radiation constant, 3.742×10^{-16} W · m^2
C_2	=	second radiation constant, 1.4388×10^{-2} m · K
F	=	geometrical coefficient related to the target geometric position
G	=	general calibration coefficient of the system, V · m^2/W
M	=	total radiation energy of the specimen surface, W/m^2
M_1	=	emissive radiation energy of the specimen surface, W/m^2
M_2	=	reflection of the specimen surface, W/m^2
P	=	coefficient of the optical system
R	=	gain of the amplifier, V/A
T_1	=	temperature of the specimen, K
T_2	=	temperature of the flame, K
V	=	voltage, V
X	=	geometrical coefficient related to the specimen, the flame, and the optical detector
α	=	air–fuel equivalence ratio
ε_1	=	emissivity of the target surface
ε_2	=	emissivity of the flame
λ_2	=	wavelength, m
τ	=	photoelectric sensitivity of the photodiodes, A/W

Introduction

RADIATION pyrometers have been widely applied in industry. With typical measurement methods, one-color and two-color pyrometry mainly considers the emission of the target surface, or introduces some simplification or correction according to the reflection of the environment radiation source on the measured surface in classical methods.[1,2] In some cases, the error may be a little large, however, because of the radiation complexity of the surface, for example, the front blade of a gas turbine, the inner surface of a combustion chamber, and so forth. The main difficulties are the existence of the radiation from the environment and the uncertain emissivity of the surface whose condition varies with temperature, oxidation level, and so forth.[3] As a simulation of typical cases in industry, the object to be studied in this paper was a metal specimen located at the outlet of a combustion chamber. More accurate temperature measurements were expected using the new method by reducing the simplification, reformulating the equation group, and rebuilding the measurement system to eliminate the complex effects.

Pyrometry Model and Experimental Setup

The target studied is a metal specimen located at the outlet of a combustion chamber. It was heated by the high-temperature fume and reflected the radiation from the combustion flame and the other components in the chamber, as shown in Fig. 1. The total radiation energy M of the specimen surface is mostly composed of two parts: the specimen emission M_1 and the specimen reflection M_2 from the flame radiation in the combustion chamber. The reflection on the specimen surface from the other components in the chamber can be neglected because of their temperature is lower.[4] It is supposed that the radiation characteristics of the emission of the specimen are similar to that of a gray body among the selected narrow wavelength band,[4] namely, $\varepsilon_1 = \varepsilon_1(T_1)$. It is also supposed that there is only one environment radiation source, which can also be considered as a gray body among the wavelengths applied in the experiment.[5] The gases at the sight path of the detector are transparent, while the air–fuel equivalence ratio $\alpha > 1$ among the same wavelength bands. Thus, we can obtain the basic equation of M_i at a given wavelength λ_i according to the simplified Planck's law:

$$M_i = M_{i1} + M_{i2} = \varepsilon_1 \frac{C_1 \lambda_i^{-5}}{\exp[C_2/(\lambda_i T_1)]} + (1 - \varepsilon_1) \frac{\varepsilon_2 X C_1 \lambda_i^{-5}}{\exp[C_2/(\lambda_i T_2)]} \tag{1}$$

Because we are concerned with only T_1, in the final analysis, there are only four unknowns in the equation, ε_1, T_1, $\varepsilon_2 X$, and T_2, that must be solved within four equations for four wavelengths. Therefore four wavelengths in the infrared region, 1.0, 1.52, 2.3, and 3.56 μm, were

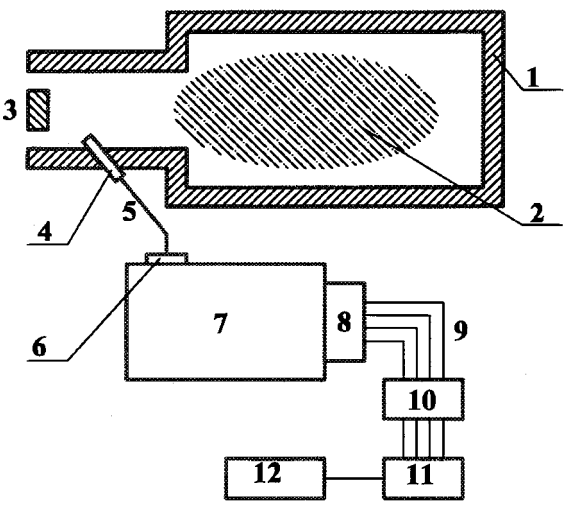

Fig. 1 Combustion chamber, specimen installation, and experimental system: combustion chamber, 1; flame, 2; specimen, 3; optical detector, 4; optical fiber, 5; entrance slit, 6; spectrometer, 7; magazine, 8; wires, 9; amplifiers, 10; A/D converter, 11; and personal computer, 12.

Received 24 May 2000; revision received 21 July 2000; accepted for publication 27 July 2000.

*Professor, Thermophysics Institute, Department of Engineering Mechanics; zhaowh@mail.tsinghua.edu.cn.

†Ph.D. Student, Thermophysics Institute, Department of Engineering Mechanics.

‡Engineer, Thermophysics Institute, Department of Engineering Mechanics.

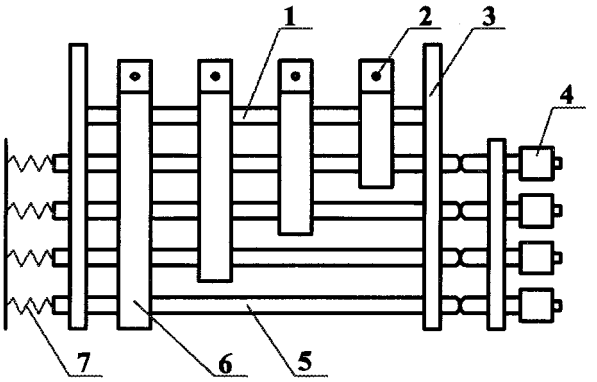

Fig. 2 Device (unit 8 in Fig. 1) to locate and detect up to four wavelengths at the exit window of the grating spectrometer: aligning rod, 1; receiving slit, 2; supporting frame, 3; micrometer screw, 4; rail, 5; sliding block, 6; and spring, 7.

separately selected to build an equation group. Absorption spectrum bands of carbon dioxide, carbon monoxide, and vapor were avoided in wavelength selection.[6]

If the radiation characteristics of the specimen are not close to that of a gray body, corrections must be introduced into the equations. Based on the typical metal, the emissivity is a decreasing function of the wavelength.[3,7] Considering that the range of the selected wavelengths was quite wide, the emissivity of the surface was multiplied by a correction coefficient less than 1.0 at the longer wavelengths.

The experimental pyrometer system has been built based on the described model. The pyrometer system is shown in Fig. 1. The specimen is installed at the position described earlier, and the detector, which collects the total radiation of the specimen, is installed in the wall of the outlet of the chamber. To obtain the radiation energy of the target at selected wavelengths, the image of the target is formed on the inlet of the optical fiber through the lens installed in the optical detector, and then transmitted to a grating spectrometer (Fig. 1). Unit 8 of Fig. 1 is designed to locate up to four wavelengths at the exit window of the spectrometer, with four high-performance photodiodes and the adjustment system installed inside, as shown in Fig. 2. The photodiodes are installed behind the receiving slits separately, and their positions can be finely adjusted by the micrometer screws. The output of the photodiodes is amplified before being transmitted to the A/D sampler. The digital results are processed by the personal computer system subsequently.

The radiation energy M_i is converted to voltage V_i through the optical detector, optical fiber, spectrometer, photodiode, and amplifier for each wavelength. It can be written as

$$V_i = (M_i/F) \times A \times P_i \times \tau_i \times R_i \qquad (2)$$

where F and A depend on the geometrical relationship between the specimen and the optical detector, P_i and τ_i are the only functions of the wavelength among the variables in Eq. (1) and can be considered to be constant for given wavelength. R_i can be also considered as a constant. Thus, Eq. (2) can be simplified to $V_i = M_i \times G_i$. G_i is calibrated by the standard tungsten strip lamp before the experiment. During calibration, there is a geometrical relationship between the tungsten strip lamp detector and the specimen detector. The value of M_i of the specimen can be calculated easily via G_i in the experiment from the voltage sampled by the A/D system.

The structure of the optical detector is shown in Fig. 3. The optical detector consists of two stainless steel concentric tubes. A sapphire lens is installed in the front of the inner tube. The tubes and the lens were cooled by a nitrogen stream, which can be considered optical transparence for radiation. The radiation inlet end of the optical fiber was installed in the inner tube.

The target point was located at the front surface of the specimen, where a type K thermal couple was embedded to contrast with the new pyrometer system.

Table 1 Comparison of pyrometer and thermocouple results

Experiment	Thermal couple, °C	Pyrometer, °C	Error, %
1	1060	1039	1.98
2	1060	1050	0.94
3	1065	1037	2.63
4	1065	1049	1.50
5	1065	1065	0
6	1100	1096	0.37
7	1110	1049	5.50
8	1140	1112	2.46
9	1150	1093	4.96

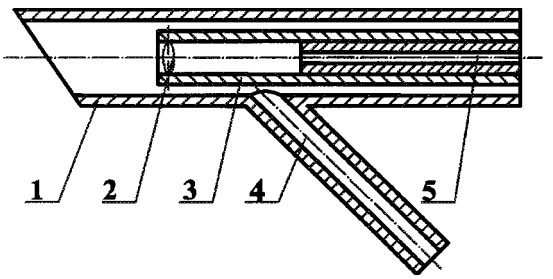

Fig. 3 Structure of the optical detector: outer tube, 1; lens, 2; inner tube, 3; nitrogen inlet, 4; and optical fiber, 5.

Results

The Newton iterative method was utilized to process the experimental data, and the initial values were provided by the negative-slope method. Some simplifications were introduced to the computational method in the actual experiments. The absolute error was less than 5%, as shown in Table 1, which compares the results obtained by the new measurement system with those of the thermocouple.

Conclusion

A new infrared multiwavelength temperature diagnostics method is presented and proven by experiment. The results of the new pyrometer system are compared with those of a classical thermocouple. Corrections must be introduced to the emissivity when the radiation characteristics of the target are not the same as that of a gray body. This new temperature measurement system can be utilized to make the surface temperature determinations in many actual industrial cases that are similar to that in the experiment described in this paper. It is suitable not only to measure the mean temperature of the specimen, but also to obtain the temperature distribution of the specimen surface if coordinated with another scan mechanism. Furthermore, it has important significance for high-speed and real-time temperature measurement and control in complex conditions.

References

[1] Foley, G. M., Morse, M. S., and Cezairliyan, A., "Two-Color Microsecond Pyrometer for 2000 to 6000 K," *Temperature, Its Measurement and Control in Science and Industry*, edited by J. F. Schooley, Vol. 5, American Inst. of Physics, New York, 1984, pp. 447–452.

[2] Anselmi-Tamburini, U., Campari, G., and Spinolo, G., "A Two-Color Spatial-Scanning Pyrometer for the Determination of Temperature Profiles in Combustion Synthesis Reactions," *Review of Scientific Instruments*, Vol. 66, No. 10, 1995, pp. 5006–5014.

[3] Leigh, J. R., *Temperature Measurement and Control*, Peter Peregrinus, London, 1988, Chap. 5.

[4] Lu, P., "Development of Four-Wavelength Radiation Pyrometer for Turbine Blades," M.S. Dissertation, Dept. of Engineering Mechanics, Tsinghua Univ., Beijing, 1995.

[5] Lefebvre, A. H., "Flame Radiation in Gas Turbine Combustion Chambers," *International Journal of Heat and Mass Transfer*, Vol. 27, No. 9, 1984, pp. 1493–1510.

[6]Ferriso, C. C., Ludwig, C. B., and Boynton, F. P., "Total Emissivity of Hot Water Vapor-I. High Pressure Limit," *International Journal of Heat and Mass Transfer*, Vol. 9, No. 9, 1966, pp. 853–864.
[7]Ge, S., and Na, H., *Heat Radiation Characters and Measurement*, Science Press, Beijing, 1989, Chap. 6.

Computational Algorithm for Thermodynamic Properties of Air to Extreme Temperatures and Pressures

C. Thames,* D. Kelly,* and J. E. Lyne†
University of Tennessee, Knoxville, Tennessee 37996

Introduction

THE current study was motivated by the need for an easily applied computational method to determine the thermodynamic properties of extremely high-temperature air. This need arose during our investigations of the atmospheric entry of large meteors. These entry bodies' trajectories are significantly effected by aerothermal ablation, and a reasonable estimate of the ablation rates requires a knowledge of the thermodynamic state of the shock layer. Previous investigators have published widely used curve fits for the thermodynamic properties of high-temperature air.[1–4] The works of Tannehill and Mugge[1] and Srinivasan et al.[2] extend to 25,000 K and 1000 atm pressure, whereas the original curve fits of Gupta et al. extended to approximately 30,000 K and 100 atm pressure.[3] Reference 4 extended Gupta's curve fits to a maximum of 1000 atm pressure and 32,600 K. Whereas these methods are sufficient to allow the calculation of equilibrium shock layer temperatures for meteors entering Earth's atmosphere at speeds up to about 20 km/s, most comets enter at velocities between 20 and 30 km/s (Ref. 5). Hence, a rapid computational method that extends to more extreme conditions is needed.

Methodology

The derivation of the desired computational algorithm was made possible by the use of thermodynamic data developed and reported by the Chance Vought Research Center in the early 1960s.[6] The thermodynamic properties in the Chance Vought Research Center report were calculated for a gas mixture model that included 30 species (up to the fifth level of ionization for nitrogen, the sixth level for oxygen, and the eighth level for argon), whereas the data used to develop previously published curve fits accounted for only 11 species.[3,4] The higher number of species considered in the Chance Vought Research Center study allows the range of applicability to extend from 3,000 to 100,000 K and from a density of $1.2(10^{-6})$ kg/m^3 to approximately 70 kg/m^3 (Fig. 1). Unfortunately, the data in the report were presented only in graphical form, and the computer models used to produce the document are no longer in existence. This is in marked contrast to the work of Refs. 1–3, which present both plotted data and computer curve fits designed for the rapid calculation of thermodynamic properties. Therefore, to use the Chance Vought Research Center data in our meteor entry studies, it was necessary to develop an algorithm to accurately calculate the desired data over a very wide range of conditions. The method devised uses well over 1500 data points read from the published plots. To fit this large quantity of data accurately, a surface fit interpolation subroutine known as ITPLBV[7] was employed. ITPLBV is well suited for the required task because it is a bivariate routine (one designed to evaluate parameters that are functions of two independent variables) and uses local procedures. (The term local procedures refers to an approach in which only known data points near the desired point are used in the interpolation, rather than all of the known data points.) This was appropriate in our case because thermodynamic data can vary by as much as 10 orders of magnitude over the range analyzed. The interpolation routine develops a set of bicubic polynomials where

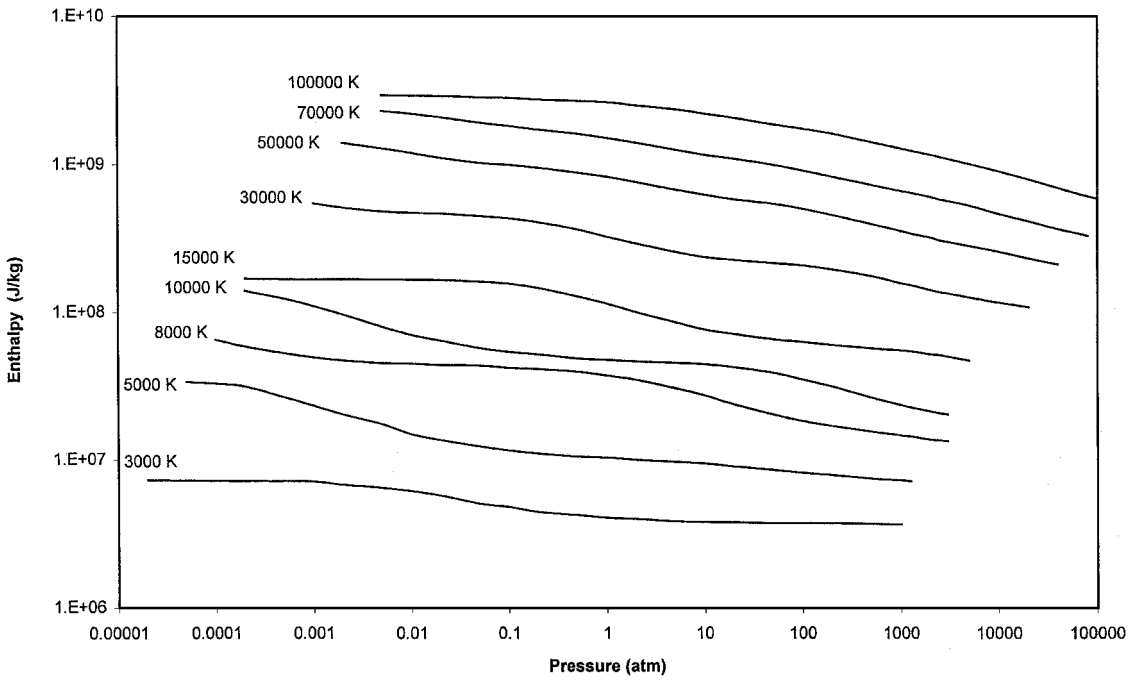

Fig. 1 Range of Chance Vought Research Center data.

Received 21 October 1999; revision received 10 September 2000; accepted for publication 3 October 2000.

*Graduate Student, Department of Mechanical and Aerospace Engineering and Engineering Science.
†Associate Professor, Department of Mechanical and Aerospace Engineering and Engineering Science. Member AIAA.